2020 59th IEEE Conference on Decision and Control (CDC)
Jeju Island, Republic of Korea, December 14-18, 2020

Lateral Vibration Suppression of a Disturbed Mining Cable Elevator with Flexible Guideways

Ji Wang, Shu-Xia Tang* and Miroslav Krstic

***Abstract*— In an ultra-deep mining cable elevator, the guideway consists of several tensioned cables from the surface to thousands of meters underground. The interaction dynamics between the cage and the flexible guideway is approximate as a spring-damping system, and the cage is subject to external disturbances. Lateral vibration suppression of the mining cable elevator is addressed in this paper, where an adaptive output-feedback boundary controller is designed for coupled hyperbolic PDEs with spatially-varying coefficients and on a time-varying domain, of which the uncontrolled boundary is coupled by an ODE subject to uncertain disturbances. The asymptotic convergence to zero of the ODE state and the boundedness of the PDE states are proved via Lyapunov analysis. The performance of the proposed controller on lateral vibration suppression of a mining cable elevator is verified in the numerical simulation.**

I. INTRODUCTION

A mining cable elevator is used to transport a cage loaded with the minerals and miners via cables for thousands of meters between the underground and the surface. The undesirable mechanical vibrations are often caused in the high-speed operation, because of the stretching and contracting abilities of cables. It would not only increase the risk of cable fracture but also cause discomfort or injury to miners. Active vibration control [18]-[20] is one economical way to suppress vibrations because the main structure of the mining elevator doesn't need to be changed. The cage is always subject to uncertain airflow disturbances [19], which should be considered in the control system design.

The objective is to design a control law at the top of a vibrational cable with a time-varying length to regulate the disturbed cage (payload) at the bottom. The vibrational cable is described as coupled transport PDEs which are from rewriting a second-order hyperbolic PDE in Riemann coordinates [20]. Many authors have contributed to boundary control of coupled transport PDEs for the past ten years, such as [1], [2], [3], [4], [5], [6], [8], [10], [11], [12], [13], [15], [16]. Considering the payload at the bottom of the cable, the plant becomes a coupled transport PDE system coupled with an ODE at the uncontrolled boundary. Boundary control of the type of this system was also studied in [9], [14], [17], [20].

The rest of the paper is organized as follows. The lateral dynamics of the mining cable elevator is built in Sec. II.

*Corresponding author.
J. Wang and M. Krstic are with the Department of Mechanical and Aerospace Engineering, University of California, San Diego, La Jolla, CA 92093-0411, USA (e-mail: jiwang9024@gmail.com;krstic@ucsd.edu).
S.-X. Tang is with the Department of Mechanical Engineering, Texas Tech University, Lubbock, TX 79409, USA (e-mail: shuxia.tang@ttu.edu).

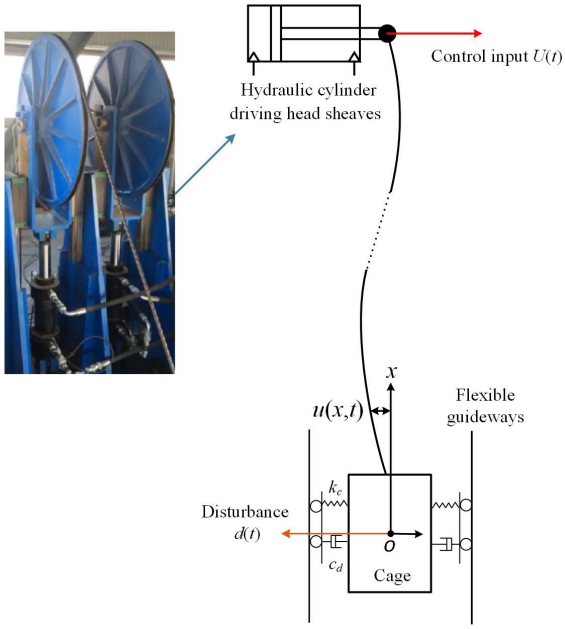

Fig. 1. Lateral vibration control of a mining cable elevator with viscoelastic guideways.

The adaptive output-feedback control law is presented in Sec. III. Under the proposed controller, the proof of the lateral vibration displacement and velocity of the cage being asymptotically convergent to zero is given via Lyapunov analysis in Sec. IV. The conclusion and future work are presented in Sec. VI.

II. PROBLEM FORMULATION

A. Original plant

Fig. 1 depicts a mining cable elevator with a disturbed cage moving along flexible guideways. The lateral vibration dynamics of the whole system is built as follows, in which the flexible guideways are approximated as a viscoelastic guide, i.e., a spring-damping system [22], [23]:

$$\dot{X}(t) = \bar{A}X(t) + \bar{B}u_x(0,t) + B_1 d(t), \tag{1}$$

$$\rho u_{tt}(x,t) = T(x)u_{xx}(x,t) - \bar{c}u_t(x,t) + T'(x)u_x(x,t), \tag{2}$$

$$u_t(0,t) = CX(t), \tag{3}$$

$$-T(l(t))u_x(l(t),t) = \bar{U}(t), \tag{4}$$

for $x \in [0, l(t)], t \in [0, \infty)$, where $l(t)$ is the time-varying length of the cable, i.e., hoisting motion of the cage, and x denotes position coordinates along the cable in a moving coordinate system associated with $l(t)$ where the origin is

located at the cage. The PDE state $u(x,t)$ denotes distributed lateral vibration displacements along the cable and the ODE state

$$X(t) = [u(0,t), u_t(0,t)]^T \tag{5}$$

describes the lateral displacement and velocity of the cage, with matrices $\bar{A}, \bar{B}, B_1, C$ being

$$\bar{A} = \begin{bmatrix} 0 & 1 \\ \frac{-k_c}{M_c} & \frac{-c_d}{M_c} \end{bmatrix}, \bar{B} = \begin{bmatrix} 0 \\ g \end{bmatrix}, \tag{6}$$

$$B_1 = \begin{bmatrix} 0 \\ \frac{1}{M_c} \end{bmatrix}, C = [0,2]. \tag{7}$$

$T(x) = M_c g + x\rho g$ is static tension along the cable with ρ being linear density of the cables, M_c being the total hoisted mass and g being gravitational acceleration. $\bar{c}$ is the material damping coefficient of the steel cables. The coefficients k_c, c_d are the equivalent stiffness and damping coefficients of the viscoelastic guide. $\bar{U}(t)$ is the lateral control force provided by the hydraulic actuator at the head sheave to be designed. The modeling process refers to [7], changing the pinned boundary condition in [7] as Neumann actuation, removing the control force at the boundary payload and adding a spring force with the coefficient k_c from the viscoelastic guide at the payload.

Assumption 1: The hoisting trajectory $l(t)$ has following two properties: 1) $l(t)$ is bounded by the the total length of the cable L, i.e., $0 < l(t) \leq L$. 2) The hoisting velocity $\dot{l}(t)$ is bounded by

$$|\dot{l}(t)| < \min_{0\leq x\leq L} \left\{ \sqrt{T(x)/\rho} \right\}.$$

Assumption 2: The uncertain external disturbance $d(t)$ is of the general harmonic form as

$$d(t) = \sum_{j=1}^{N} [a_j \cos(\theta_j t) + b_j \sin(\theta_j t)], \tag{8}$$

where the integer N is arbitrary. The frequencies $\theta_j,\ j \in \{1,2,\cdots,N\}$ are known and arbitrary constants. The amplitudes a_j, b_j are unknown constants bounded by the known and arbitrary constants $\bar{a}_j, \bar{b}_j$, i.e., $a_j \in [0,\bar{a}_j],\ b_j \in [0,\bar{b}_j]$.

Note that Assumption 2 can model most periodic disturbance signals since N is arbitrary and can be chosen sufficiently large.

B. Reformed plant

Applying the Riemann transformations:

$$z(x,t) = u_t(x,t) - \sqrt{\frac{T(x)}{\rho}} u_x(x,t), \tag{9}$$

$$w(x,t) = u_t(x,t) + \sqrt{\frac{T(x)}{\rho}} u_x(x,t), \tag{10}$$

the original model (1)-(4) is reformed as the following coupled transported PDEs-ODE:

$$\dot{X}(t) = AX(t) + Bw(0,t) + B_1 d(t), \tag{11}$$

$$z(0,t) = CX(t) - w(0,t), \tag{12}$$

$$z_t(x,t) = -q(x) z_x(x,t) + c_1(x) z(x,t) + c_2(x) w(x,t), \tag{13}$$

$$w_t(x,t) = q(x) w_x(x,t) + c_1(x) z(x,t) + c_2(x) w(x,t), \tag{14}$$

$$w(l(t),t) = U(t) + z(l(t),t), \tag{15}$$

where

$$A = \begin{pmatrix} 0 & 1 \\ \frac{-k_c}{M_c} & \frac{-c_d - \sqrt{M_c \rho g}}{M_c} \end{pmatrix},\ B = \begin{pmatrix} 0 \\ \sqrt{\frac{\rho g}{M_c}} \end{pmatrix}, \tag{16}$$

$$q(x) = \sqrt{\frac{T(x)}{\rho}},\ c_1(x) = \frac{-\bar{c}}{2\rho} - \frac{T'(x)}{4\sqrt{\rho T(x)}},$$

$$c_2(x) = \frac{-\bar{c}}{2\rho} + \frac{T'(x)}{4\sqrt{\rho T(x)}}.$$

The new control signal is

$$U(t) = \frac{-2\bar{U}(t)}{\sqrt{\rho T(l(t))}}, \tag{17}$$

which is to be designed based on (11)-(15).

Note that from Assumption 1,

$$|\dot{l}(t)| < \min_{0\leq x\leq L} \{q(x)\}. \tag{18}$$

Also, from (5), (9), (10), we have the relationship

$$u(x,t) = \int_0^x \frac{1}{2} \sqrt{\frac{\rho}{T(x)}} (w(x,t) - z(x,t)) dx + C_1 X(t), \tag{19}$$

where $C_1 = [1,0]$.

III. Output-feedback adaptive control system

A. Control law

We propose the following adaptive output-feedback control law

$$\begin{aligned} U(t) = 2\Big[& -u_t(l(t),t) - \Gamma(l(t),t) Z(t) + D(l(t)) X(t) \\ & + \int_0^{l(t)} \bar{\Upsilon}(l(t),y)(\hat{z}(y,t) + \Gamma_1(y,t) Z(t)) dy \\ & + \int_0^{l(t)} \check{\Upsilon}(l(t),y)(\hat{w}(y,t) + \Gamma(y,t) Z(t)) dy \\ & + \int_0^{l(t)} \hat{N}(l(t),y) \Big(\hat{w}(y,t) + \Gamma(y,t) Z(t) \\ & - \int_0^y \bar{\Upsilon}(y,\sigma)(\hat{z}(\sigma,t) + \Gamma_1(\sigma,t) Z(t)) d\sigma \\ & - \int_0^y \check{\Upsilon}(y,\sigma)(\hat{w}(\sigma,t) + \Gamma(\sigma,t) Z(t)) d\sigma \Big) dy \Big], \end{aligned} \tag{20}$$

which is constructed only depending on two measurements $X(t)$ and $u_t(l(t),t)$. $X(t)$, i.e., the vibration displacement and velocity of the cage in the mining cable elevator, are obtained by the acceleration sensor placed at the cage plus

twice integration [18]. Similarly, $u_t(l(t),t)$, i.e., the lateral vibration velocity at the top of the cable, are obtained by the acceleration sensor at the head sheave with an integration. Multiplying by $\frac{-\sqrt{\rho T(l(t))}}{2}$ according to (17), then $U(t)$ (20) can be converted into the lateral control force $\bar{U}(t)$, i.e., the control input in the original wave PDE model. Other components in (20) are illustrated as follows.

B. Definitions of components in the control law

1) $Z(t),\hat{z}(x,t),\hat{w}(x,t)$: The vector $Z(t)$ is defined as

$$Z(t)=[\cos(\theta_1 t),\sin(\theta_1 t),\cdots,\cos(\theta_N t),\sin(\theta_N t)]^T. \quad (21)$$

$\hat{z}(x,t),\hat{w}(x,t)$ are states of the PDE state observer built as

$$\hat{z}(0,t)=CX(t)-\hat{w}(0,t), \quad (22)$$

$$\hat{z}_t(x,t)=-q(x)\hat{z}_x(x,t)+c_1(x)\hat{z}(x,t)+c_2(x)\hat{w}(x,t) + \Phi_2(x,t)(u_t(l(t),t)-\frac{1}{2}U(t)-\hat{z}(l(t),t)), \quad (23)$$

$$\hat{w}_t(x,t)=q(x)\hat{w}_x(x,t)+c_1(x)\hat{z}(x,t)+c_2(x)\hat{w}(x,t) + \Phi_3(x,t)(u_t(l(t),t)-\frac{1}{2}U(t)-\hat{z}(l(t),t)), \quad (24)$$

$$\hat{w}(l(t),t)=U(t)+u_t(l(t),t)-\frac{1}{2}U(t). \quad (25)$$

Note that $u_t(l(t),t)-\frac{1}{2}U(t)=u_t(l(t),t)-\sqrt{\frac{T(l(t))}{\rho}}u_x(l(t),t)=z(l(t),t)$. The observer gains are

$$\Phi_2(x,t)=\dot{l}(t)\bar{\phi}(x,l(t))-q(l(t))\bar{\phi}(x,l(t)), \quad (26)$$

$$\Phi_3(x,t)=\dot{l}(t)\bar{\psi}(x,l(t))-q(l(t))\bar{\psi}(x,l(t)). \quad (27)$$

In practice $\bar{\phi}(x,y),\check{\phi}(x,y),\bar{\psi}(x,y),\check{\psi}(x,y)$ can be solved from the following four transport PDEs by using the finite difference method,

$$-c_1(x)-(q(x)+q(x))\bar{\psi}(x,x)=0, \quad (28)$$

$$\bar{\psi}(0,y)+\bar{\phi}(0,y)=0, \quad (29)$$

$$q(x)\check{\psi}_x(x,y)+\check{\psi}_y(x,y)q(y)+c_1(x)\check{\phi}(x,y) + (c_2(x)-c_2(y))\check{\psi}(x,y)+q'(y)\check{\psi}(x,y)=0, \quad (30)$$

$$-q(y)\bar{\psi}_y(x,y)+q(x)\bar{\psi}_x(x,y)-q'(y)\bar{\psi}(x,y) + c_1(x)\bar{\phi}(x,y)+(c_2(x)-c_1(y))\bar{\psi}(x,y)=0, \quad (31)$$

$$\check{\phi}_y(x,y)q(y)-q(x)\check{\phi}_x(x,y)+\check{\phi}(x,y)q'(y) + (c_1(x)-c_2(y))\check{\phi}(x,y)+c_2(x)\check{\psi}(x,y)=0, \quad (32)$$

$$-q(x)\bar{\phi}_x(x,y)-q(y)\bar{\phi}_y(x,y)-c_1(y)\bar{\phi}(x,y) + c_1(x)\bar{\phi}(x,y)+c_2(x)\bar{\psi}(x,y)-q'(y)\bar{\phi}(x,y)=0, \quad (33)$$

$$\check{\psi}(0,y)+\check{\phi}(0,y)=0, \quad (34)$$

$$\check{\phi}(x,x)(q(x)+q(x))-c_2(x)=0, \quad (35)$$

which are obtained by using the backstepping design.

2) $\Gamma_1(x,t),\Gamma(x,t),\hat{N}(x,y),\bar{\Upsilon}(x,y),\check{\Upsilon}(x,y),D(x)$: Defining

$$\zeta(x,t)^T=[\Gamma(x,t),\Gamma_1(x,t)], \quad (36)$$

where the superscript T means transposition, $\zeta(x,t)$ is the solution of the ODE

$$\zeta_x(x,t)+\bar{\mathscr{A}}(x)\zeta(x,t)=0, \quad (37)$$

where

$$\bar{\mathscr{A}}(x)=\begin{pmatrix}-q(x)&0\\0&q(x)\end{pmatrix}^{-1}\begin{pmatrix}A_z-c_2(x)&-c_1(x)\\-c_2(x)&A_z-c_1(x)\end{pmatrix},$$

and

$$A_z=\mathrm{diag}\left(\begin{pmatrix}0&-\theta_1\\\theta_1&0\end{pmatrix},\cdots,\begin{pmatrix}0&-\theta_N\\\theta_N&0\end{pmatrix}\right). \quad (38)$$

The initial condition of the ODE (37) is

$$\zeta(0,t)=\begin{pmatrix}\Gamma(0,t)\\\Gamma_1(0,t)\end{pmatrix} =\begin{pmatrix}\hat{a}_1(t),\hat{b}_1(t),\cdots,\hat{a}_N(t),\hat{b}_N(t)\\-\hat{a}_1(t),-\hat{b}_1(t),\cdots,-\hat{a}_N(t),-\hat{b}_N(t)\end{pmatrix}, \quad (39)$$

where $\hat{a}_j(t),\hat{b}_j(t),\ j\in\{1,\cdots,N\}$, are adaptive estimations of a_j,b_j, defined by

$$\dot{\hat{a}}_j(t)=\mathrm{Proj}_{[0,\bar{a}_j]}\left(\tau_{1j}(t),\hat{a}_j(t)\right), \quad (40)$$

$$\dot{\hat{b}}_j(t)=\mathrm{Proj}_{[0,\bar{b}_j]}\left(\tau_{2j}(t),\hat{b}_j(t)\right). \quad (41)$$

$\mathrm{Proj}_{[m,M]}$ is the standard projection operator given by

$$\mathrm{Proj}_{[m,M]}(r,p)=\begin{cases}0, & \text{if } p=m \text{ and } r<0,\\0, & \text{if } p=M \text{ and } r>0,\\r, & \text{else.}\end{cases}$$

The bounds $\bar{a}_j,\bar{b}_j$ are defined in Sec. II, and $\tau_{1j}(t),\tau_{2j}(t)$ are defined as

$$\tau_{1j}(t)=\gamma_{aj}\frac{\left(2X^TPB_1-r_a\int_0^{l(t)}e^{\delta x}\hat{\eta}(x,t)D(x)B_1dx\right)\cos(\theta_j t)}{1+\Omega(t)}, \quad (42)$$

$$\tau_{2j}(t)=\gamma_{bj}\frac{\left(2X^TPB_1-r_a\int_0^{l(t)}e^{\delta x}\hat{\eta}(x,t)D(x)B_1dx\right)\sin(\theta_j t)}{1+\Omega(t)}, \quad (43)$$

which are obtained from Lyapunov analysis in the proof of Lemma 2. The components in (42)-(43) are illustrated in the rest of this section. The signals $\hat{\eta}(\cdot,t)$ and $\hat{\alpha}(\cdot,t)$ included in $\Omega(t)$ which will be shown later, are represented by the observer states $\hat{w}(x,t),\hat{z}(x,t)$ through the inverses of the following invertible transformations:

$$\hat{v}(x,t)=\hat{w}(x,t)+\Gamma(x,t)Z(t), \quad (44)$$

$$\hat{s}(x,t)=\hat{z}(x,t)+\Gamma_1(x,t)Z(t), \quad (45)$$

$$\hat{\alpha}(x,t)=\hat{s}(x,t)-\int_0^x\bar{\lambda}(x,y)\hat{s}(y,t)dy-\int_0^x\check{\lambda}(x,y)\hat{v}(y,t)dy, \quad (46)$$

$$\hat{\beta}(x,t)=\hat{v}(x,t)-\int_0^x\bar{\Upsilon}(x,y)\hat{s}(y,t)dy-\int_0^x\check{\Upsilon}(x,y)\hat{v}(y,t)dy, \quad (47)$$

$$\hat{\eta}(x,t)=\hat{\beta}(x,t)-\int_0^x\hat{N}(x,y)\hat{\beta}(y,t)dy-D(x)X(t), \quad (48)$$

where $\bar{\lambda}(x,y),\check{\lambda}(x,y),\bar{\Upsilon}(x,y),\check{\Upsilon}(x,y)$ are solved from the following four transport PDEs:

$$c_2(x)-(q(x)+q(x))\check{\lambda}(x,x)=0, \tag{49}$$
$$\check{\lambda}(x,0)q(0)+\bar{\lambda}(x,0)q(0)=0, \tag{50}$$
$$\check{\lambda}_y(x,y)q(y)-q(x)\check{\lambda}_x(x,y)-\bar{\lambda}(x,y)c_2(y) + (q'(y)+c_1(x)-c_2(y))\check{\lambda}(x,y)=0, \tag{51}$$
$$\bar{\lambda}_y(x,y)q(y)+q(x)\bar{\lambda}_x(x,y)+\check{\lambda}(x,y)c_1(y) + \bar{\lambda}(x,y)(q'(y)+c_1(y)-c_1(x))=0, \tag{52}$$
$$c_1(x)+(q(x)+q(x))\bar{\Upsilon}(x,x)=0, \tag{53}$$
$$\check{\Upsilon}(x,0)q(0)+\bar{\Upsilon}(x,0)q(0)=0, \tag{54}$$
$$\check{\Upsilon}_y(x,y)q(y)+q(x)\check{\Upsilon}_x(x,y)-\bar{\Upsilon}(x,y)c_2(y) + (q'(y)+c_2(x)-c_2(y))\check{\Upsilon}(x,y)=0, \tag{55}$$
$$\bar{\Upsilon}_y(x,y)q(y)-q(x)\bar{\Upsilon}_x(x,y)+\check{\Upsilon}(x,y)c_1(y) + \bar{\Upsilon}(x,y)(q'(y)+c_1(y)-c_2(x))=0, \tag{56}$$

and $\hat{N}(x,y),D(x)$ are solved from the following transport PDE-ODE system:

$$D(0)=K, \tag{57}$$
$$-q(x)D'(x)+D(x)(A-c_2(x)) + \bar{\Upsilon}(x,0)q(0)C-\int_0^x \hat{N}(x,y)\bar{\Upsilon}(y,0)q(0)Cdy=0, \tag{58}$$
$$q(y)\hat{N}_y(x,y)+q(x)\hat{N}_x(x,y)+q'(y)\hat{N}(x,y)=0, \tag{59}$$
$$q(0)\hat{N}(x,0)-D(x)B=0. \tag{60}$$

$\Omega(t)$ in (42)-(43) is defined as

$$\Omega(t)=X^TPX(t)+\frac{1}{2}r_a\int_0^{l(t)}e^{\delta x}\hat{\eta}(x,t)^2dx + \frac{1}{2}r_b\int_0^{l(t)}e^{-\delta x}\hat{\alpha}(x,t)^2dx. \tag{61}$$

According to (16), (A,B) is stabilizable. Choose a control gain vector K such that $A_m=A+BK$ is a Hurwitz matrix. Let the matrix $P=P^T>0$ be the unique solution to the following Lyapunov equation

$$PA_m+A_m^TP=-Q \tag{62}$$

for some $Q=Q^T>0$.

The positive constant δ should be chosen to satisfy

$$\delta>\max\left\{\frac{2\overline{c_2}+\overline{q'}}{\underline{q}},\frac{2\overline{c_1}+1+\overline{q'}}{\underline{q}}\right\}, \tag{63}$$

where

$$\underline{q}=\min_{0\le x\le L}\{q(x)\},\quad \overline{q'}=\max_{0\le x\le L}\{|q'(x)|\}, \tag{64}$$
$$\overline{c_1}=\max_{0\le x\le L}\{|c_1(x)|\},\quad \overline{c_2}=\max_{0\le x\le L}\{|c_2(x)|\}. \tag{65}$$

Positive constants r_a,r_b are chosen to satisfy

$$r_b<\frac{\frac{3}{4}\lambda_{\min}(Q)}{q(0)|\bar{D}|^2+\frac{q(0)^2}{2}L\bar{J}^2|C|^2}, \tag{66}$$
$$r_a>\frac{2}{q(0)}\left(q(0)r_b-\frac{8}{\lambda_{\min}(Q)}|PB|^2\right), \tag{67}$$

where

$$\bar{J}=\max_{0\le x\le L}\{|\bar{\lambda}(x,0)|\}, \tag{68}$$
$$\bar{D}=\max_{0\le x\le L}\{|C-D(x)|\}. \tag{69}$$

$\lambda_{\min}$ denotes the minimal eigenvalues of the corresponding matrices. The positive update gains γ_{aj},γ_{bj} in (42)-(43) should be chosen sufficiently small according to Lyapunov analysis.

C. Design philosophy of the control law

The adaptive backstepping boundary control is designed based on the state observer (22)-(25). Then, we apply the transformations (44)-(48) to attenuate the unmatched disturbance, remove couplings in the PDE domain and make the state matrix of the ODE Hurwitz. We achieve a target system (77)-(81) including adaptive estimation errors. For the right boundary condition of the target system to hold, the boundary controller including the adaptive laws is derived, where the adaptive laws are built from the Lyapunov analysis based on the target system.

IV. Stability of the closed-loop system

The following lemma shows the effectiveness of the observer (22)-(25).

Lemma 1: Considering the observer (22)-(25) with the observer gains (26)-(27), $z(x,t)-\hat{z}(x,t),w(x,t)-\hat{w}(x,t)$ become zero after $t=\frac{2L}{\min_{0\le x\le L}\{q(x)\}}$.

Proof: Defining the observer error state as

$$(\tilde{z}(x,t),\tilde{w}(x,t))=(z(x,t),w(x,t))-(\hat{z}(x,t),\hat{w}(x,t)), \tag{70}$$

the resulting observer error system is converted to the following target observer error system

$$\tilde{\alpha}(0,t)=-\tilde{\beta}(0,t), \tag{71}$$
$$\tilde{\alpha}_t(x,t)=-q(x)\tilde{\alpha}_x(x,t)+c_1(x)\tilde{\alpha}(x,t), \tag{72}$$
$$\tilde{\beta}_t(x,t)=q(x)\tilde{\beta}_x(x,t)+c_2(x)\tilde{\beta}(x,t), \tag{73}$$
$$\tilde{\beta}(l(t),t)=0 \tag{74}$$

via the invertible backtepping transformation

$$\tilde{z}(x,t)=\tilde{\alpha}(x,t)-\int_x^{l(t)}\bar{\phi}(x,y)\tilde{\alpha}(y,t)dy - \int_x^{l(t)}\check{\phi}(x,y)\tilde{\beta}(y,t)dy, \tag{75}$$
$$\tilde{w}(x,t)=\tilde{\beta}(x,t)-\int_x^{l(t)}\bar{\psi}(x,y)\tilde{\alpha}(y,t)dy - \int_x^{l(t)}\check{\psi}(x,y)\tilde{\beta}(y,t)dy, \tag{76}$$

where the observer gains (26)-(27) and the conditions of $\bar{\phi}(x,y),\check{\phi}(x,y),\bar{\psi}(x,y),\check{\psi}(x,y)$ (28)-(35) are used. According to the stability result in [11] and the invertibility of the backstepping transformations, the proof of this lemma is completed. ■

Through the transformations (44)-(48), the observer (22)-(25) with (11) written as $\dot{X}(t) = AX(t) + B(\hat{w}(0,t) + \tilde{w}(0,t)) + B_1 d(t)$, is converted to the final target system:

$$\dot{X}(t) = A_m X(t) + B\hat{\eta}(0,t) + B_1\tilde{d}(t), \tag{77}$$

$$\hat{\alpha}(0,t) = (C - D(0))X(t) - \hat{\eta}(0,t), \tag{78}$$

$$\begin{aligned}\hat{\alpha}_t(x,t) &= -q(x)\hat{\alpha}_x(x,t) + c_1(x)\hat{\alpha}(x,t)\\ &- \bar{\lambda}(x,0)q(0)CX(t) + \Bigg(\Gamma_{1t}(x,t)\\ &- \int_0^x \bar{\lambda}(x,y)\Gamma_{1t}(y,t)dy - \int_0^x \check{\lambda}(x,y)\Gamma_t(y,t)dy\Bigg)Z(t),\end{aligned} \tag{79}$$

$$\begin{aligned}\hat{\eta}_t(x,t) &= q(x)\hat{\eta}_x(x,t) + c_2(x)\hat{\eta}(x,t)\\ &+ \Bigg[\Gamma_t(x,t) - \int_0^x \check{\Upsilon}(x,y)\Gamma_t(y,t)dy - \int_0^x \bar{\Upsilon}(x,y)\Gamma_{1t}(y,t)dy\\ &+ \int_0^x \hat{N}(x,y)\Bigg(\int_0^y \check{\Upsilon}(y,z)\Gamma_t(z,t)dz + \int_0^y \bar{\Upsilon}(y,z)\Gamma_{1t}(z,t)dz\\ &+ \Gamma_t(y,t)\Bigg)dy\Bigg]Z(t) - D(x)B_1\tilde{d}(t),\end{aligned} \tag{80}$$

$$\hat{\eta}(l(t),t) = 0, \tag{81}$$

where

$$\tilde{d}(t) = \sum_{j=1}^{N}[\tilde{a}_j(t)\cos(\theta_j t) + \tilde{b}_j(t)\sin(\theta_j t)],$$

and $\tilde{a}_j(t) = a_j - \hat{a}_j(t)$, $\tilde{b}_j(t) = b_j - \hat{b}_j(t)$. Note that the output injections $\tilde{z}(l(t),t) = u_t(l(t),t) - \frac{1}{2}U(t) - \hat{z}(l(t),t)$ and $\tilde{w}(l(t),t)$ are regarded as zero in the above conversion, i.e., the state-feedback design, and then the separation principle will be verified and applied in the stability analysis of the resulting closed-loop system, by recalling Lemma 1 which shows the observer errors vanish in a finite time which only depends on the plant parameters. The conditions (36)-(39), (49)-(60) are obtained from matching (22)-(25) and (77)-(81) through (44)-(48). The following lemma shows the asymptotical stability of the target system.

Lemma 2: For any initial data $(\hat{\alpha}(\cdot,0), \hat{\eta}(\cdot,0), X(0)) \in L^2(0,L) \times L^2(0,L) \times \mathbb{R}^2$, the target system (77)-(81) is asymptotically stable in the sense of

$$\lim_{t\to\infty}(\|\hat{\alpha}(\cdot,t)\| + \|\hat{\eta}(\cdot,t)\| + |X(t)|) = 0. \tag{82}$$

Proof: Consider a Lyapunov functional

$$V(t) = \ln(1+\Omega(t)) + \sum_{j=1}^{N}\frac{1}{2\gamma_{aj}}\tilde{a}_j(t)^2 + \sum_{j=1}^{N}\frac{1}{2\gamma_{bj}}\tilde{b}_j(t)^2. \tag{83}$$

Taking the time derivative of (83), recalling (18), (63), (66)-(67), inserting the adaptive laws (40)-(43), choosing small sufficiently γ_{aj}, γ_{bj}, through a lengthy calculation, we obtain

$$\begin{aligned}\dot{V}(t) \le \frac{-\bar{\lambda}_a}{1+\Omega}\Bigg(&|X(t)|^2 + \hat{\eta}(0,t)^2 + \|\hat{\eta}(\cdot,t)\|^2\\ &+ \hat{\alpha}(l(t),t)^2 + \|\hat{\alpha}(\cdot,t)\|^2\Bigg) \le 0\end{aligned} \tag{84}$$

for some positive $\bar{\lambda}_a$. We in further have boundedness of $\frac{d}{dt}|X(t)|^2$, $\frac{d}{dt}\|\hat{\eta}(\cdot,t)\|^2$, $\frac{d}{dt}\|\hat{\alpha}(\cdot,t)\|^2$ along (77)-(81). Finally, integrating (84) from 0 to ∞, it follows that $|X(t)|$, $\|\hat{\alpha}(\cdot,t)\|$, $\|\hat{\eta}(\cdot,t)\|$ are square integrable. Following Barbalat's Lemma that $|X(t)|$, $\|\hat{\alpha}(\cdot,t)\|$, $\|\hat{\eta}(\cdot,t)\|$ tend to zero as $t \to \infty$. Due to the space limit, the details in this proof are omitted. ■

TABLE I

PHYSICAL PARAMETERS OF THE MINING CABLE ELEVATOR.

Parameters (units)	Values
Initial length L (m)	300
Final length (m)	2700
Cable linear density ρ (kg/m)	8. 5
Total hoisted mass M_c (kg)	20000
Gravitational acceleration g (m/s^2)	9.8
Maximum hoisting velocities $\bar{v}_{\max}$ (m/s)	20
Total hoisting time t_f(s)	150
Cable material damping coefficient $\bar{c}$	0.4
Viscoelastic guideway equivalent damping coefficient c_d	0.4
Viscoelastic guideway equivalent stiffness coefficient k_d	1500

Using Lemmas 1-2, we obtain the main result of this paper, which physically shows the lateral vibration displacement and velocity of the cage are convergent to zero under the proposed controller.

Theorem 1: For any initial data $(z(\cdot,0), w(\cdot,0), X(0)) \in L^2(0,L) \times L^2(0,L) \times \mathbb{R}^2$, the closed-loop system including the plant (11)-(15), the observer (22)-(25), the adaptive update laws (42)-(43) and the control law (20), has the following properties:

1) The ODE state $X(t)$ in the closed-loop system is asymptotically convergent to zero in the sense of

$$\lim_{t\to\infty}|X(t)| = 0. \tag{85}$$

2) The PDE states in the closed-loop system are ultimately uniformly bounded in the sense of the norm

$$\|z(\cdot,t)\| + \|w(\cdot,t)\|. \tag{86}$$

Proof: Recalling the asymptotic stability result proved in Lemma 2, property 1) is obtained straightforwardly. Considering the invertibility and continuity of the backstepping transformations (46)-(47), (48), we obtain the asymptotic convergence to zero of $\|\hat{v}(\cdot,t)\| + \|\hat{s}(\cdot,t)\|$. Applying Cauchy-Schwarz inequality into (44)-(45), we obtain the ultimate uniform boundedness of $\|\hat{w}(\cdot,t)\|$, $\|\hat{z}(\cdot,t)\|$. Recalling Lemma 1 and (70), applying the separation principle verified by the independent stability results of the observer error system in Lemma 1 and the state-feedback loop in Lemma 2, property 2) is obtained. ■

V. SIMULATION

The parameters of the mining cable elevator are shown in Tab. I. The hoisting velocity curve $l(t)$ and the according velocity $\dot{l}(t)$ are shown in Fig. 2. The disturbance applied at the cage is given as

$$d(t) = 15\cos\left(\frac{\pi}{8}t\right) + 20\sin\left(\frac{\pi}{8}t\right), \tag{87}$$

where the amplitudes $15, 20$ are assumed to be unknown. The initial lateral offset of the cage is defined as 0.2m and the initial vibration velocity is defined as zero. Applying the proposed controller, and the traditional PD controller, the comparing results of the lateral vibration displacement and

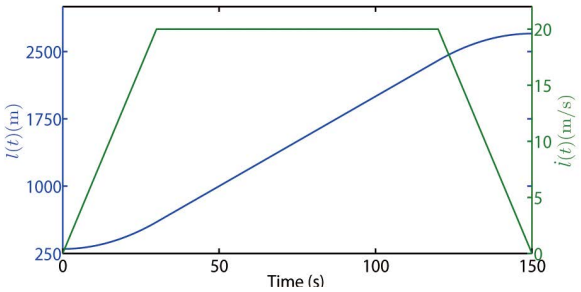

Fig. 2. Hoisting trajectory $l(t)$ and hoisting velocity $\dot{l}(t)$.

velocity of the cage are shown in Figs. 3-4, where we observe both the proposed adaptive controller and the traditional PD controller can reduce the lateral vibrations of the cage in the descending operation of the mining cable elevator with flexible guideways. Even though the performance of proposed adaptive controller is worse than the PD controller at the beginning due to the adaptive learning transient, the proposed controller can reduce the lateral vibration displacements and velocities to a smaller range around zero as time goes on under the uncertain disturbance (87). It verifies the proposed adaptive controller has the better performance on lateral vibration suppressions.

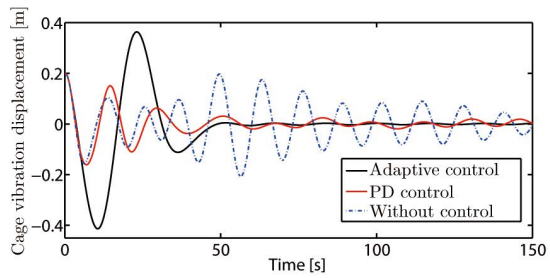

Fig. 3. Lateral vibration displacement of the cage.

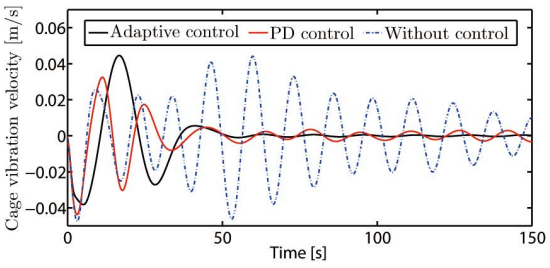

Fig. 4. Lateral vibration velocity of the cage.

VI. Conclusion and Future Work

We propose an adaptive output-feedback controller applied at the head sheave to suppress the lateral vibrations of an ultra-deep mining cable elevator with flexible guideways which are approximate as a spring-damping system, and the cage is subject to uncertain external disturbances. The simulation results show the proposed adaptive controller effectively suppresses the lateral vibration displacements and velocities of the cage in the descending mining cable elevator. In future works, the hydraulic actuator dynamics and input delay will be incorporated into the control design.

References

[1] O.M. Aamo, "Disturbance rejection in 2×2 linear hyperbolic systems," *IEEE Trans. Autom. Control*, 58(2013), pp. 1095-1106.

[2] H. Anfinsen and O. M. Aamo, " Disturbance rejection in general heterodirectional 1-D linear hyperbolic systems using collocated sensing and control", *Automatica*, 76, pp.230-242, 2017.

[3] H. Anfinsen and O. M. Aamo, " Adaptive output-feedback stabilization of linear 2×2 hyperbolic systems using anti-collocated sensing and control", *Systems & Control Letters*, 104, pp.86-94, 2017.

[4] H. Anfinsen and O.M. Aamo, "Adaptive control of linear 2×2 hyperbolic systems", *Automatica*, 87, pp.69-82, 2018.

[5] H. Anfinsen, and O.M. Aamo, *Adaptive Control of Hyperbolic PDEs*, 2019. Springer.

[6] J.M. Coron, R. Vazquez, M. Krstic and G. Bastin, " Local exponential H^2 stabilization of a 2×2 quasilinear hyperbolic system using backstepping", *SIAM Journal on Control and Optimization*, 51(3), pp.2005-2035, 2013.

[7] H. Canbolat, D. Dawson, C. Rahn and S. Nagarkatti, " Adaptive boundary control of out-of-plane cable vibration", *Journal of Applied Mechanics*, 65, pp.963-969, 1998.

[8] J. Deutscher, "Finite-time output regulation for linear 2×2 hyperbolic systems using backstepping". *Automatica*, 75, pp.54-62, 2017.

[9] J. Deutscher, N. Gehring and R. Kern "Output feedback control of general linear heterodirectional hyperbolic PDE-ODE systems with spatially-varying coefficients". *Int. J. Control*, 92, pp.2274-2290, 2019.

[10] J. Deutscher, "Output regulation for general linear heterodirectional hyperbolic systems with spatially-varying coefficients". *Automatica*, 85, pp.34-42, 2017.

[11] L. Hu, F. Di Meglio, R. Vazquez and M. Krstic, "Control of homodirectional and general heterodirectional linear coupled hyperbolic PDEs", *IEEE Trans. Autom. Control*, 61(11), pp.3301-3314, 2016.

[12] P.-O. Lamare, N. Bekiaris-Liberis, "Control of 2×2 linear hyperbolic systems: backstepping-based trajectory generation and PI-based tracking", *Systems & Control Letters*, 86, pp. 24-33, 2015.

[13] F. Di Meglio, R. Vazquez and M. Krstic, " Stabilization of a system of $n+1$ coupled first-order hyperbolic linear PDEs with a single boundary input". *IEEE Trans. Autom. Control*, 58, pp. 3097-3111, 2013.

[14] F. Di Meglio, F. Bribiesca, L. Hu and M. Krstic, " Stabilization of coupled linear heterodirectional hyperbolic PDE-ODE systems". *Automatica*, 87, pp.281-289, 2018.

[15] S.-X. Tang and M. Krstic, "Sliding mode control to the stabilization of a linear 2×2 hyperbolic system with boundary input disturbance," *In Proc. American Control Conference*, pp. 1027-1032, Portland, Oregon, USA, 2014.

[16] R. Vazquez, M. Krstic and J.M. Coron, "Backstepping boundary stabilization and state estimation of a 2×2 linear hyperbolic system", In Decision and Control and European Control Conference (CDC-ECC), 50th IEEE Conference on (pp. 4937-4942), 2011.

[17] J. Wang and M. Krstic, "Vibration suppression for coupled wave PDEs in deep-sea construction", *IEEE Trans. Control Syst. Technol.*, DOI: 10.1109/TCST.2020.3009660, 2020.

[18] J. Wang, S. Koga, Y. Pi and M. Krstic, "Axial vibration suppression in a PDE model of ascending mining cable elevator", *ASME Journal of Dynamic Systems, Measurement and Control*, 140(2018), 111003.

[19] J. Wang, S.-X. Tang, Y. Pi and M. Krstic, "Exponential anti-collocated regulation of the disturbed cage in a wave PDE-modeled ascending cable elevator", *Automatica*, 95, pp. 122-136, 2018.

[20] J. Wang, Y. Pi and M. Krstic, "Balancing and suppression of oscillations of tension and cage in dual-cable mining elevators", *Automatica*, 98, pp. 223-238, 2018.

[21] J. Wang, S.-X. Tang and M. Krstic, "Adaptive output-feedback control of torsional vibration in off-shore rotary oil drilling systems", *Automatica*, 111, pp.108640, 2020.

[22] Y. Terumichi, M. Ohtsuka, M. Yoshizawa, Nonstationary vibrations of a string with time-varying length and a mass-spring system attached at the lower end, *Nonlinear Dyn.* 12 (1997) 39-55.

[23] W.D. Zhu, G.Y. Xu, Vibration of elevator cables with small bending stiffness, *J. Sound Vib.* 263 (2003) 679-699.